This is the author's version of an article that has been published in this journal. Changes were made to this version by the publisher prior to publication.
The final version of record is available at http://dx.doi.org/10.1109/TMAG.2013.2294945

Instantaneous Power Balance in Finite-Element Simulation of Electrical Machines

Paavo Rasilo[1,2], Lauri Perkkiö[3], Antti Hannukainen[3], Bishal Silwal[1], Timo Eirola[3], Antero Arkkio[1]

[1]Aalto University, Dept. of Electrical Engineering, P.O. Box 13000, FI-00076 Aalto, Finland
[2]Ghent University, Dept. of Electrical Energy, Systems and Automation, Sint-Pietersnieuwstraat, 41, B-9000, Ghent, Belgium
[3]Aalto University, Dept. of Mathematics and Systems Analysis, P.O. Box 11000, FI-00076 Aalto, Finland

Abstract—Conservation of power in time-stepping finite-element (FE) simulation of electrical machines is studied. We propose a method for accurately obtaining the instantaneous time derivative of the FE solution, from which the instantaneous eddy-current losses and the rate-of-change of the magnetic field energy are calculated. The method is shown to be consistent with different time-integration schemes, unlike the typically-used backward-difference (BWD) approximation, which is only accurate if the BWD method is also used for the time integration. We first formulate the FE equations for a locked-rotor induction machine as a differential-algebraic equation (DAE) system. An approach called the collocation method is then used to derive the BWD, trapezoidal (TR) and implicit midpoint (IM) integration rules in order to show how these methods approximate the solution in time. We then differentiate the constraint equations of the DAE to form a system from which the time derivative of the solution can be solved. The obtained derivative is shown to satisfy the power balance exactly in the collocation points. In case of the TR rule, the losses calculated with the proposed method are shown to be less sensitive to the time-step length than ones obtained with the BWD approximation for the time derivatives. The collocation approach also allows studying the power balance continuously during the time step.

***Index Terms*—Collocation method, eddy currents, electrical machines, field energy, finite element methods, power balance.**

I. Introduction

TIME-STEPPING finite-element (FE) analysis is widely used for the prediction of torques, currents, power losses and vibrations of electrical machines. While the two former are needed in the energy conversion process of the machine, the two latter are related to dissipation of energy and should usually be minimized. During the past 20 years, increasingly complex models for more accurate computation of the power losses and magnetomechanical interaction have been developed. Naturally, in order to obtain accurate results, the errors caused in the power balance by the FE model and the applied time-stepping scheme should be minimized.

The instantaneous power balance of an electrical machine can be written as

$$P_{\text{in}}(t) = P_{\text{out}}(t) + P_{\text{loss}}(t) + \frac{dW_{\text{mag}}(t)}{dt}, \qquad (1)$$

in which part of the input power P_{in} is transformed as output power P_{out}, part is consumed as losses P_{loss} and the rest changes the energy W_{mag} stored in the magnetic field of the machine. For the powers predicted by an ideal model, (1) should be exactly satisfied at all instants of time. However, numerical time-integration schemes typically cause errors in the instantaneous and average power balances, especially, when the nonlinear material properties of the ferromagnetic core are considered [1].

Although the possibilities of deriving global quantities from FE solutions using energy balance considerations have been known for long [2], [3], a review on the literature also shows a recent interest in the numerical power and energy balance studies in both circuit [4], [5] and FE simulations [6]-[15]. In [7]-[10] the power balance was applied to verify the proposed iron-loss models for both 2-D and 3-D analysis of electrical machines. The energy conservation properties of the most commonly used backward-difference (BWD) and trapezoidal (TR) time-integration methods were discussed in [11]. The authors concluded the TR rule to be *power balanced* in case of a linear RL circuit. Strictly speaking, however, they did not focus on the instantaneous power balance (1) but rather on the average reactive power over one excitation cycle in a steady state. Thus the discussion was more related to the *energy balanced* properties of the TR rule [12], which was finally applied to solve a transient FE problem with a simple eddy-current loss model for core laminations. In [13], the authors discussed the calculation of the instantaneous active and reactive powers from a coupled field-circuit FE formulation for an inductor, while [1], [14] and [15] focused on calculating the electromagnetic torque of a rotating machine from the power balance. In [1], the TR rule was applied for the time integration, but only the average torque over each time step was considered. On the other hand, the authors of [15] calculated the instantaneous torque at the end points of the time steps, but performed the time integration using the BWD method, which itself is known to be energy-consuming even in the linear case [1], [11], [12].

As a conclusion from the literature review, general methods for calculating the instantaneous power balance consistently with different time-integration schemes have not been discussed so far. In this paper, we derive a general method for calculation of the instantaneous power balance of the FE solution for an induction machine. Since inductive power consumption is related to time-varying currents and magnetic fields, the problem of calculating the instantaneous power balance of the FE solution is reduced to the problem of

Manuscript received August 27, 2013. Corresponding author: P. Rasilo (e-mail: paavo.rasilo@alumni.aalto.fi).
Digital Object Identifier inserted by IEEE

obtaining the instantaneous time derivative of the solution accurately. The time derivative can then be used to calculate the instantaneous eddy-current losses and the rate-of-change of the magnetic field energy.

Below, we first briefly describe the main problems related to obtaining the instantaneous time derivative of the FE solution. As a test case, we study a locked-rotor induction machine, in which mechanical power transfer does not occur, and which thus avoids problems related to the accuracy of torque computation. The FE system for the machine is formulated as a differential-algebraic equation (DAE) system in which the differential equations are coupled to constraint equations which do not include the time derivatives of the variables. We then use an approach called the collocation method to derive the BWD and TR time-integration rules in order to know the time instants at which the DAE system is satisfied, and to understand how the different integration rules approximate the solution in time. Finally, we show that the instantaneous time derivative of the solution can be obtained by differentiating the constraint equations of the DAE system independently of the chosen time-integration rule. The ability of the method to satisfy the power balance in the collocation points is demonstrated in case of the TR and implicit midpoint (IM) rules.

II. Problem Statement and Test Case

A. Differential-Algebraic Equations

Typically, the FE solution regions in electrical machines include domains with both conducting and nonconducting regions. The spatial FE discretization of the magnetic field problem in these regions leads to DAE systems. For example, consider the following eddy-current problem with the magnetic vector potential $\boldsymbol{A}$ as the variable:

$$\nabla \times \left(\nu \nabla \times \boldsymbol{A} \right) + \sigma \frac{\partial \boldsymbol{A}}{\partial t} = \boldsymbol{J}_{\mathrm{s}} \, . \tag{2}$$

Here ν is the magnetic reluctivity and σ the electrical conductivity which is zero in nonconducting regions (subscript n) and nonzero in conducting regions (c). $\boldsymbol{J}_{\mathrm{s}}$ includes the source currents which are assumed to be nonzero only in the nonconducting regions. Spatial discretization of (2) results in a DAE system

$$\begin{bmatrix} \boldsymbol{S}_{\mathrm{nn}} & \boldsymbol{S}_{\mathrm{nc}} \\ \boldsymbol{S}_{\mathrm{cn}} & \boldsymbol{S}_{\mathrm{cc}} \end{bmatrix} \begin{bmatrix} \boldsymbol{a}_{\mathrm{n}} \\ \boldsymbol{a}_{\mathrm{c}} \end{bmatrix} + \begin{bmatrix} \boldsymbol{0} & \boldsymbol{0} \\ \boldsymbol{0} & \boldsymbol{T}_{\mathrm{cc}} \end{bmatrix} \frac{d}{dt} \begin{bmatrix} \boldsymbol{a}_{\mathrm{n}} \\ \boldsymbol{a}_{\mathrm{c}} \end{bmatrix} = \begin{bmatrix} \boldsymbol{j}_{\mathrm{s}} \\ \boldsymbol{0} \end{bmatrix}, \tag{3}$$

in which $\boldsymbol{j}_{\mathrm{s}}$ includes the source terms, vectors $\boldsymbol{a}$ include the nodal values of the vector potential, submatrices $\boldsymbol{S}$ are the magnetic stiffness matrices, and submatrix $\boldsymbol{T}_{\mathrm{cc}}$ the damping matrix related to the eddy currents.

What distinguishes the DAE system from a system of ordinary differential equations (ODE) is that the total damping matrix multiplying the time derivative of the solution has empty rows and columns, and thus it cannot be inverted to directly solve the time derivative from (3). The equations for which the damping part is zero, i.e., the ones in the upper part of 2, are called *constraint equations*. The *differentiation index* of the DAE is defined as the number of times the constraint equations have to be differentiated in order to transform the DAE into an ODE. For (3), this index is one. Although the numerical solution of a general high-index DAE system can be rather difficult [16], [17], the solution for (3) can be straightforwardly obtained by applying a numerical time-integration scheme similar to the ones used for the solution of ODEs. In this paper, we focus on the BWD, TR and IM time-integration rules (the TR rule being sometimes also called the Crank-Nicolson method), which, for a general ODE $d\boldsymbol{x} / dt = \boldsymbol{f}(\boldsymbol{x},t)$, can be written, respectively, as

$$\boldsymbol{x}_{\mathrm{end}} = \boldsymbol{x}_{\mathrm{beg}} + \boldsymbol{f}\left(\boldsymbol{x}_{\mathrm{end}}, t_{\mathrm{end}}\right) \Delta t \, , \tag{4}$$

$$\boldsymbol{x}_{\mathrm{end}} = \boldsymbol{x}_{\mathrm{beg}} + \frac{\boldsymbol{f}\left(\boldsymbol{x}_{\mathrm{beg}}, t_{\mathrm{beg}}\right) + \boldsymbol{f}\left(\boldsymbol{x}_{\mathrm{end}}, t_{\mathrm{end}}\right)}{2} \Delta t \, , \tag{5}$$

$$\boldsymbol{x}_{\mathrm{end}} = \boldsymbol{x}_{\mathrm{beg}} + \boldsymbol{f}\left(\frac{\boldsymbol{x}_{\mathrm{beg}} + \boldsymbol{x}_{\mathrm{end}}}{2}, \frac{t_{\mathrm{beg}} + t_{\mathrm{end}}}{2} \right) \Delta t \, , \tag{6}$$

in which subscripts 'beg' and 'end' denote the solution at the beginning and end of a time step, and Δt is the time-step length. In case of DAEs, regardless of the chosen time-integration method, it has to be ensured that the initial conditions given for $\boldsymbol{a}_{\mathrm{n}}$ and $\boldsymbol{a}_{\mathrm{c}}$ are *consistent*, meaning that they satisfy the constraint equations.

B. Induction-Machine Model

As a test case to the power balance studies, a voltage-supplied star-connected locked-rotor 37-kW induction machine (IM) is considered. The FE mesh, rated data and some dimensions of the machine are given in Fig. 1 and Table I. The voltage-supplied IM is a reasonable application for the problem due to the coupling of the FE equations not only to the circuit equations of the stator winding but also to the rotor cage equations. On the other hand, locking the rotor ensures that no mechanical power transfer occurs which allows neglecting possible errors in the computation of the electromagnetic torque from the FE solution.

The FE and circuit equations for the induction machine are derived following the approach of [18]. For a 2-D case, the vector potential $\boldsymbol{A} = A\boldsymbol{u}_{\mathrm{z}}$ is perpendicular to the solution region (xy-plane). Coupling to the stator voltage equations is relatively straightforward and thus only the rotor cage voltage equations are discussed here in more detail. The potential differences over the rotor bars are

$$\boldsymbol{u}_{\mathrm{r}} = -l R_{\mathrm{bar}} \boldsymbol{C} \frac{d\boldsymbol{a}_{\mathrm{c}}}{dt} + R_{\mathrm{bar}} \boldsymbol{i}_{\mathrm{r}} + 2 L_{\mathrm{eb}} \frac{d\boldsymbol{i}_{\mathrm{r}}}{dt} \, , \tag{7}$$

in which l, R_{bar}, and L_{eb} are the axial length of the machine, the resistance of the rotor bar and the inductance of the bar end outside the core region, respectively, and the elements of matrix $\boldsymbol{C}$ are obtained as integrals over the rotor bars:

$$C_{ij} = -\frac{1}{l} \int_{\Omega_{\mathrm{bar}\,i}} \sigma N_j \left(x, y\right) d\Omega \, . \tag{8}$$

The bar currents $\boldsymbol{i}_{\mathrm{r}}$ are obtained as differences of the adjacent end ring currents $\boldsymbol{i}_{\mathrm{sc}}$, which can be written as (p. 42 of [18])

$$\boldsymbol{i}_{\mathrm{r}} = -\boldsymbol{M}^{\mathrm{T}}\boldsymbol{i}_{\mathrm{sc}}. \tag{9}$$

The voltages over the end-ring segments are caused by the segment resistances and inductances R_{sc} and L_{sc}, respectively, and equal half of the differences of the bar potentials:

$$\boldsymbol{u}_{\mathrm{sc}} = R_{\mathrm{sc}}\boldsymbol{i}_{\mathrm{sc}} + L_{\mathrm{sc}}\frac{d\boldsymbol{i}_{\mathrm{sc}}}{dt} = \frac{1}{2}\boldsymbol{M}\boldsymbol{u}_{\mathrm{r}}. \tag{10}$$

Substituting (9) into (7) yields

$$\boldsymbol{u}_{\mathrm{r}} = -lR_{\mathrm{bar}}\boldsymbol{C}\frac{d\boldsymbol{a}_{\mathrm{c}}}{dt} - R_{\mathrm{bar}}\boldsymbol{M}^{\mathrm{T}}\boldsymbol{i}_{\mathrm{sc}} - 2L_{\mathrm{eb}}\boldsymbol{M}^{\mathrm{T}}\frac{d\boldsymbol{i}_{\mathrm{sc}}}{dt}, \tag{11}$$

which together with (10) describes the rotor cage voltage equations. In principle the potentials $\boldsymbol{u}_{\mathrm{r}}$ could be easily eliminated from the equations by multiplying (11) by $\boldsymbol{M}$ and substituting $\boldsymbol{M}\boldsymbol{u}_{\mathrm{r}}$ into (10). However, choosing the currents as the variables results in an integro-differential formulation for the source of the field, which significantly increases the computational burden of the model. We thus prefer to keep both the bar voltages and end-ring currents in the equations and calculate the source for the field as $\boldsymbol{C}^{\mathrm{T}}\boldsymbol{u}_{\mathrm{r}}$.

The full FE system coupled to the circuit equations can now be written as

$$\boldsymbol{S}(\boldsymbol{x})\boldsymbol{x} + \boldsymbol{T}\frac{d\boldsymbol{x}}{dt} = \boldsymbol{v}, \tag{12}$$

in which the variable (column) vector $\boldsymbol{x} = [\boldsymbol{a}_{\mathrm{n}}\,;\, \boldsymbol{a}_{\mathrm{c}}\,;\, \boldsymbol{i}_{\mathrm{s}}\,;\, \boldsymbol{u}_{\mathrm{r}}\,;\, \boldsymbol{i}_{\mathrm{sc}}]$ includes the nodal values of the vector potential A, the stator currents, as well as the rotor voltages and currents. The source vector $\boldsymbol{v} = [\boldsymbol{0}\,;\,\boldsymbol{0}\,;\,\boldsymbol{v}_{\mathrm{s}}\,;\,\boldsymbol{0}\,;\,\boldsymbol{0}]$ includes stator line-to-line voltages. The stiffness and damping matrices, respectively, are

$$\boldsymbol{S}(\boldsymbol{x}) = \begin{bmatrix} \boldsymbol{S}_{\mathrm{nn}}(\boldsymbol{a}_{\mathrm{n}}) & \boldsymbol{S}_{\mathrm{nc}}(\boldsymbol{a}) & (\boldsymbol{KD})^{\mathrm{T}} & \cdot & \cdot \\ \boldsymbol{S}_{\mathrm{cn}}(\boldsymbol{a}) & \boldsymbol{S}_{\mathrm{cc}} & \cdot & \boldsymbol{C}^{\mathrm{T}} & \cdot \\ \cdot & \cdot & R_{\mathrm{s}}\boldsymbol{KK}^{\mathrm{T}} & \cdot & \cdot \\ \cdot & \cdot & \cdot & \boldsymbol{I} & R_{\mathrm{bar}}\boldsymbol{M}^{\mathrm{T}} \\ \cdot & \cdot & \cdot & \frac{1}{2}\boldsymbol{M} & -R_{\mathrm{sc}}\boldsymbol{I} \end{bmatrix} \tag{13}$$

$$\boldsymbol{T} = \begin{bmatrix} \cdot & \cdot & \cdot & \cdot & \cdot \\ \cdot & \boldsymbol{T}_{\mathrm{cc}} & \cdot & \cdot & \cdot \\ l\boldsymbol{KD} & \cdot & L_{\mathrm{ew}}\boldsymbol{KK}^{\mathrm{T}} & \cdot & \cdot \\ \cdot & lR_{\mathrm{bar}}\boldsymbol{C} & \cdot & \cdot & 2L_{\mathrm{eb}}\boldsymbol{M}^{\mathrm{T}} \\ \cdot & \cdot & \cdot & \cdot & -L_{\mathrm{sc}}\boldsymbol{I} \end{bmatrix}. \tag{14}$$

in which the stiffness matrix depends on the solution in the nonlinear case, matrix $\boldsymbol{D}$ defines the stator flux linkage and gives the source for the field from the stator currents, while $\boldsymbol{K}$ is related to the connection of the stator winding. With star connection, only two independent currents $\boldsymbol{i}_{\mathrm{s}} = \boldsymbol{i}_{\mathrm{ab}} = [i_{\mathrm{a}}\ i_{\mathrm{b}}]^{\mathrm{T}}$ are solved, $\boldsymbol{i}_{\mathrm{abc}} = \boldsymbol{K}\boldsymbol{i}_{\mathrm{ab}}$, and $\boldsymbol{v}_{\mathrm{s}} = [v_{\mathrm{ab}}\ v_{\mathrm{bc}}]^{\mathrm{T}}$. $\boldsymbol{I}$ denotes the identity matrix with its size corresponding to the number of rotor bars. To simplify the notation, it has been assumed that the stator winding nodes belong to the nonconducting regions, all the conducting regions are linear, and that the Dirichlet and periodic boundary conditions are included in the matrices.

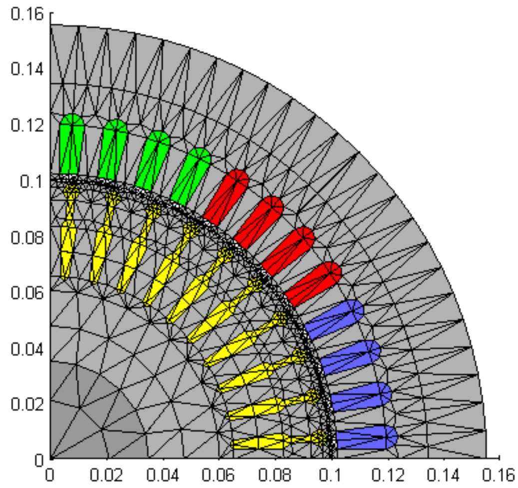

Fig. 1 FE mesh of the induction machine.

TABLE I
DATA AND DIMENSIONS OF THE INDUCTION MACHINE

Machine type	motor
Rated shaft power	37 kW
Rated voltage	400 V
Rated current	69 A
Rated frequency	50 Hz
Connection	star
Number of pole pairs	2
Stator outer diameter	310 mm
Stator inner diameter	200 mm
Air gap	0.8 mm
Number of stator slots	48
Number of rotor slots	40

C. Problems in Power-Balance Calculation

The error in the power balance of the locked-rotor machine can be written as

$$r_{\mathrm{P}} = P_{\mathrm{in}}(t) - P_{\mathrm{Cu,s}}(t) - P_{\mathrm{cage}}(t) - \frac{dW_{\mathrm{mag}}(t)}{dt}, \tag{15}$$

in which

$$P_{\mathrm{in}}(t) = i_{\mathrm{a}}(t)\big(v_{\mathrm{ab}}(t) + v_{\mathrm{bc}}(t)\big) + i_{\mathrm{b}}(t)v_{\mathrm{bc}}(t), \tag{16}$$

$$P_{\mathrm{Cu,s}}(t) = R_{\mathrm{s}}\boldsymbol{i}_{\mathrm{abc}}(t)^{\mathrm{T}}\boldsymbol{i}_{\mathrm{abc}}(t), \tag{17}$$

$$P_{\mathrm{cage}}(t) = \sum_{i=1}^{n_{\mathrm{bar}}}\int_{\Omega_i}\sigma\left(\left(\frac{\partial A(x,y,t)}{\partial t}\right)^2 - \frac{u_{\mathrm{r},i}}{l}\frac{\partial A(x,y,t)}{\partial t}\right)dxdy, \tag{18}$$

$$\frac{dW_{\mathrm{mag}}(t)}{dt} = \int_{\Omega}\nu\boldsymbol{B}(x,y,t)\cdot\frac{\partial\boldsymbol{B}(x,y,t)}{\partial t}dxdy + L_{\mathrm{ew}}\boldsymbol{i}_{\mathrm{abc}}^{\mathrm{T}}\frac{d\boldsymbol{i}_{\mathrm{abc}}}{dt}, \tag{19}$$

respectively, are the electrical input power, the resistive loss of the stator winding, the power fed into the cage, as well as the rate-of-change of the magnetic field energy in the solution region. In (18), n_{bar} denotes the number of the rotor bars and the integrations are performed over each bar Ω_i. In addition to the eddy-current losses in the core region, $P_{\mathrm{cage}}(t)$ includes the power fed to the end rings of the cage, which changes the magnetic field energy stored in the inductances L_{eb} and L_{sc} and is consumed as losses in the short-circuit ring resistances R_{sc}.

It is clear that obtaining the instantaneous values of the power terms (18) and (19) requires knowing the instantaneous values of the time derivatives of the vector potential and the stator currents. However, since the damping matrix $\boldsymbol{T}$ has empty rows, the system is clearly a DAE and the time derivative of $\boldsymbol{x}$ cannot be directly solved from (12). Thus a typical approach for the calculation of the time derivative is to apply the BWD method (4) to the numerical solution to approximate the time derivative:

$$\left(\frac{d\boldsymbol{x}}{dt}\right)_{\mathrm{end}} \approx \frac{\boldsymbol{x}_{\mathrm{end}} - \boldsymbol{x}_{\mathrm{beg}}}{\Delta t}. \tag{20}$$

However, it seems obvious that the BWD approximation for the derivative is only consistent with the BWD time-integration method, and thus errors may arise if, for example, the TR rule is applied for the time-integration. This is indeed shown in Fig. 2 which presents the powers and the power balance calculated with the BWD approximation (20) for the time derivative during the first tenth of a period after a 50-Hz, 400-V terminal voltage with 10 % of the 35th harmonic is connected to the terminals of the machine. Fig. 2 a) shows the results obtained with the BWD rule (4) for the time integration, while in b) the TR rule (5) has been used. It can be seen that the power balance is very well satisfied in a) in which the derivative approximation is consistent with the integration method. However, in b), the instantaneous error in the power balance rises close to 5 % of the input power which confirms that the BWD formula (20) doesn't yield correct results with the TR integration rule.

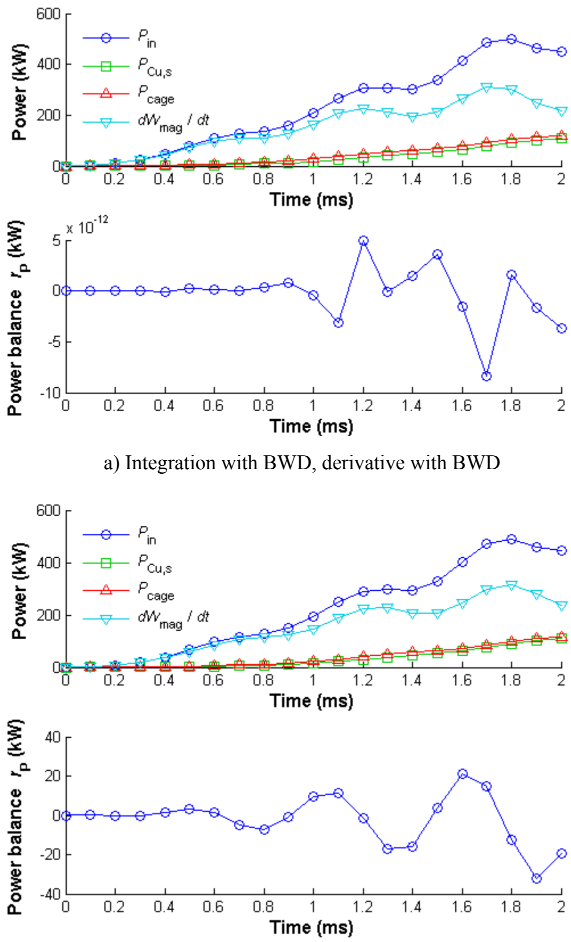

a) Integration with BWD, derivative with BWD

b) Integration with TR, derivative with BWD

Fig. 2 End-point powers and power balances for the induction machine calculated with the BWD approximation for the time derivative while using a) the BWD rule and b) the TR rule for the time integration.

The question now arises how the time derivative of the solution should be calculated when using the TR rule or, more generally, any other time integration rule for the numerical solution of (12). A possible approach is proposed next.

III. Methods

A. Collocation Method

We start by deriving a group of time-integration methods for the solution of (12) using a technique called the *collocation method* [12], [19]. The solution over a time step is approximated as an n^{th}-order polynomial:

$$\boldsymbol{x}(t) = \boldsymbol{x}_{\mathrm{beg}} + \sum_{k=1}^{n} t^k \boldsymbol{\alpha}_k , \tag{21}$$

in which $\boldsymbol{x}_{\mathrm{beg}}$ is the solution at the beginning of the time step and the (vector) coefficients $\boldsymbol{\alpha}_k$ are constants in time. For simplicity, the initial time is assumed to be zero and the end-point of the time step is Δt. Owing to the n^{th}-order approximation, we can now require (12) to be exactly satisfied at n separate time instants t_i called the *collocation points*, for which $0 \le t_1 < t_2 < \ldots < t_n \le \Delta t$. Now, by differentiating (21), multiplying with $\boldsymbol{T}$, and requiring (12) to be satisfied at the collocation points t_i, we get

$$\boldsymbol{T}\sum_{k=1}^{n} k t_i^{k-1} \boldsymbol{\alpha}_k = \boldsymbol{v}_i - \boldsymbol{S}_i \boldsymbol{x}_i , \tag{22}$$

in which

$$\boldsymbol{x}_i = \boldsymbol{x}_{\mathrm{beg}} + \sum_{k=1}^{n} t_i^k \boldsymbol{\alpha}_k , \tag{23}$$

and a short-hand notation $\boldsymbol{S}_i = \boldsymbol{S}(\boldsymbol{x}_i)$ is used for the dependence of the stiffness matrix on the solution. Combining (22) and (23) yields

$$\sum_{k=1}^{n} t_i^{k-1}\left(k\boldsymbol{T} + t_i \boldsymbol{S}_i\right)\boldsymbol{\alpha}_k = \boldsymbol{v}_i - \boldsymbol{S}_i \boldsymbol{x}_{\mathrm{beg}} , \tag{24}$$

which, when evaluated for each $i = 1, \ldots, n$, gives a system

$$\begin{bmatrix} \boldsymbol{T} + t_1 \boldsymbol{S}_1 & \cdots & t_1^{n-1}\left(n\boldsymbol{T} + t_1 \boldsymbol{S}_1\right) \\ \vdots & & \vdots \\ \boldsymbol{T} + t_n \boldsymbol{S}_n & \cdots & t_n^{n-1}\left(n\boldsymbol{T} + t_n \boldsymbol{S}_n\right) \end{bmatrix} \begin{bmatrix} \boldsymbol{\alpha}_1 \\ \vdots \\ \boldsymbol{\alpha}_n \end{bmatrix} = \begin{bmatrix} \boldsymbol{v}_1 \\ \vdots \\ \boldsymbol{v}_n \end{bmatrix} - \begin{bmatrix} \boldsymbol{S}_1 \\ \vdots \\ \boldsymbol{S}_n \end{bmatrix} \boldsymbol{x}_{\mathrm{beg}} . \tag{25}$$

In the case of an ODE system, there are no constraint equations, matrix $\boldsymbol{T}$ is invertible and $\boldsymbol{\alpha}_i$ can be solved from

(25) for any n separate collocation points. In case of a DAE, however, $\boldsymbol{T}$ has empty rows corresponding to the constraint equations, and thus the left-hand-side matrix is invertible only if $t_1 > 0$. In this case, coefficients $\boldsymbol{\alpha}_i$ are again solvable from (25), and the solution at the end point of the time-step can be calculated as

$$\boldsymbol{x}_{\text{end}} = \boldsymbol{x}_{\text{beg}} + \sum_{k=1}^{n} \Delta t^k \boldsymbol{\alpha}_k \,. \tag{26}$$

In the nonlinear case, the solution of (25) has to be iterated, e.g., with the Newton-Raphson method which requires knowing the Jacobian matrix

$$\boldsymbol{P}(\boldsymbol{x}) = \frac{d\left(\boldsymbol{S}(\boldsymbol{x})\boldsymbol{x}\right)}{d\boldsymbol{x}} = \boldsymbol{S}(\boldsymbol{x}) + \frac{d\boldsymbol{S}(\boldsymbol{x})}{d\boldsymbol{x}}\boldsymbol{x}\,. \tag{27}$$

It is obvious that if $\boldsymbol{\alpha}_i$ are solvable, the derivative of the solution can be directly calculated by differentiating (21). However, if $n > 1$ and the first collocation point is chosen to coincide with the beginning of the time step, i.e., $t_1 = 0$, the left-hand-side matrix in (25) is not invertible and $\boldsymbol{\alpha}_i$ cannot be solved. This makes it necessary to set the last collocation point to coincide with the end point of the time step, $t_n = \Delta t$, in order to know the initial value for the next step. In addition, we also know that $\boldsymbol{T\alpha}_1 = \boldsymbol{v}_{\text{beg}} - \boldsymbol{S}_{\text{beg}}\boldsymbol{x}_{\text{beg}}$, and by evaluating (22) for $i = 2, \ldots, n$ gives a system from which $\boldsymbol{T\alpha}_i$ can be solved:

$$\begin{bmatrix} 2t_2\boldsymbol{I} & \cdots & nt_2^{n-1}\boldsymbol{I} \\ \vdots & & \vdots \\ 2t_n\boldsymbol{I} & \cdots & nt_n^{n-1}\boldsymbol{I} \end{bmatrix} \begin{bmatrix} \boldsymbol{T\alpha}_2 \\ \vdots \\ \boldsymbol{T\alpha}_n \end{bmatrix} = \begin{bmatrix} \boldsymbol{v}_2 \\ \vdots \\ \boldsymbol{v}_{\text{end}} \end{bmatrix} - \begin{bmatrix} \boldsymbol{S}_2\boldsymbol{x}_2 \\ \vdots \\ \boldsymbol{S}_{\text{end}}\boldsymbol{x}_{\text{end}} \end{bmatrix} - \begin{bmatrix} \boldsymbol{T\alpha}_1 \\ \vdots \\ \boldsymbol{T\alpha}_1 \end{bmatrix}. \tag{28}$$

Now, multiplication of (23) by $\boldsymbol{T}$ and again evaluating for $i = 2, \ldots, n$ gives a system, into which the solution of $\boldsymbol{T\alpha}_i$ from (28) can be substituted. The resulting system finally allows solving for $\boldsymbol{x}_2, \ldots, \boldsymbol{x}_{\text{end}}$ without the need to know $\boldsymbol{\alpha}_i$. Finally, we point out that if $n = 1$ and $t_1 = 0$, the system is not solvable. This case corresponds to the explicit Euler or forward-difference method, which together with other explicit methods is not well applicable for the solution of DAE systems.

After the idea of the collocation method is clear, it is straightforward to show that many commonly-used implicit methods including the BWD and TR rules can be obtained by the following choices of collocation points:

backward-difference:	$n = 1,\ t_1 = \Delta t,$
trapezoidal:	$n = 2,\ t_1 = 0,\ t_2 = \Delta t,$
implicit midpoint:	$n = 1,\ t_1 = \Delta t / 2$
4-th order Gauss-Legendre:	$n = 2,\ t_{1,2} = (1 \pm 3^{-0.5})\ \Delta t / 2.$

Although the BWD and TR methods could be implemented directly using (4) and (5), the derivation with the collocation method reveals interesting facts on these methods which may otherwise be difficult to observe. First of all, we now know that the system equation (12) is satisfied in the chosen collocation points, at least in the sense of the convergence tolerance set for the nonlinear iteration. Secondly, the TR rule uses a second-order polynomial to approximate the solution in time, with the collocation points set both at the beginning and the end of the time steps. This essentially makes the first derivative of the solution continuous on the boundary between adjacent steps. On the other hand, the solution is only known in the two collocation points and thus not uniquely determined over the whole time step. Also the derivative of the solution is not known. However, if a value for the derivative in one of the collocation points can be obtained, also the solution polynomial becomes unique.

The BWD and IM rules only use a linear approximation for the solution and one collocation point either at the end or in the middle of the time step. Thus the time derivative of the solution is constant over the whole step and not continuous from one step to the other. However, the derivative is easily obtained since the only collocation coefficient $\boldsymbol{\alpha}_1$ is uniquely defined and solvable from (25).

At the end, it is emphasized that the order of the time-integration method referring to the convergence rate with respect to time-step length is not the same as the order of the polynomial used for the approximation in time. For example, the IM method uses a linear approximation for the solution in time but is a second-order method regarding the convergence.

B. Differentiation of Constraint Equations

As discussed above, the problem in obtaining the derivative of the solution mainly occurs if the first collocation point is set at the beginning of the time step (as is the case with the TR rule). In order to obtain the derivative also in these cases, we propose to differentiate the constraint equations with respect to time, which can sometimes be used to solve DAE systems [16]. In our case, the collocation method revealed that the solution is differentiable in the collocation points, if a second- or higher-order polynomial is used for the approximation in time, or if the collocation point in a linear approximation is not set and the end of the time step (corresponding to the BWD rule). Thus, differentiation of the constraint equations is allowed in the collocation points. In the locked-rotor case the stiffness matrices $\boldsymbol{S}$ only depend on time through their dependence on the solution itself, and differentiation of the first rows of (12) gives

$$\boldsymbol{L}(\boldsymbol{x})\frac{d\boldsymbol{x}}{dt} = \boldsymbol{v} - \boldsymbol{R}(\boldsymbol{x})\boldsymbol{x}\,, \tag{29}$$

in which

$$\boldsymbol{L}(\boldsymbol{x}) = \begin{bmatrix} \boldsymbol{P}_{\text{nn}}(\boldsymbol{a}) & \boldsymbol{P}_{\text{nc}}(\boldsymbol{a}) & (\boldsymbol{KD})^{\text{T}} & \cdot & \cdot \\ \cdot & \boldsymbol{T}_{\text{cc}} & \cdot & \cdot & \cdot \\ l\boldsymbol{KD} & \cdot & L_{\text{ew}}\boldsymbol{KK}^{\text{T}} & \cdot & \cdot \\ \cdot & lR_{\text{bar}}\boldsymbol{C} & \cdot & \cdot & 2L_{\text{eb}}\boldsymbol{M}^{\text{T}} \\ \cdot & \cdot & \cdot & \cdot & -L_{\text{sc}}\boldsymbol{I} \end{bmatrix}, \tag{30}$$

$$\boldsymbol{R}(\boldsymbol{x}) = \begin{bmatrix} \cdot & \cdot & \cdot & \cdot & \cdot \\ \boldsymbol{S}_{\text{cn}}(\boldsymbol{a}) & \boldsymbol{S}_{\text{cc}} & \cdot & \boldsymbol{C}^{\text{T}} & \cdot \\ \cdot & \cdot & R_{\text{s}}\boldsymbol{KK}^{\text{T}} & \cdot & \cdot \\ \cdot & \cdot & \cdot & \boldsymbol{I} & R_{\text{bar}}\boldsymbol{M}^{\text{T}} \\ \cdot & \cdot & \cdot & \frac{1}{2}\boldsymbol{M} & -R_{\text{sc}}\boldsymbol{I} \end{bmatrix}. \tag{31}$$

Here

$$\boldsymbol{P}_{\mathrm{nn}}\left(\boldsymbol{a}\right)=\boldsymbol{S}_{\mathrm{nn}}\left(\boldsymbol{a}_{\mathrm{n}}\right)+\frac{\partial\boldsymbol{S}_{\mathrm{nn}}\left(\boldsymbol{a}_{\mathrm{n}}\right)}{\partial\boldsymbol{a}_{\mathrm{n}}}\boldsymbol{a}_{\mathrm{n}}+\frac{\partial\boldsymbol{S}_{\mathrm{nc}}\left(\boldsymbol{a}_{\mathrm{n}},\boldsymbol{a}_{\mathrm{c}}\right)}{\partial\boldsymbol{a}_{\mathrm{n}}}\boldsymbol{a}_{\mathrm{c}} \quad (32)$$

and

$$\boldsymbol{P}_{\mathrm{nc}}\left(\boldsymbol{a}\right)=\boldsymbol{S}_{\mathrm{nc}}\left(\boldsymbol{a}\right)+\frac{\partial\boldsymbol{S}_{\mathrm{nc}}\left(\boldsymbol{a}_{\mathrm{n}},\boldsymbol{a}_{\mathrm{c}}\right)}{\partial\boldsymbol{a}_{\mathrm{c}}}\boldsymbol{a}_{\mathrm{c}} \quad (33)$$

are the Jacobian matrices resulting from the differentiation of the stiffness matrix with respect to the vector potential.

The left-hand-side matrix $\boldsymbol{L}(\boldsymbol{x})$ still has empty columns and is thus not yet invertible. These columns, however, are related to the time derivative of the rotor bar potential differences which are of no interest, since they do not cause losses in the machine and do not affect the other derivatives which are to be calculated. To make $\boldsymbol{L}(\boldsymbol{x})$ invertible, we can thus change it to

$$\boldsymbol{L}\left(\boldsymbol{x}\right)=\begin{bmatrix}\boldsymbol{P}_{\mathrm{nn}}\left(\boldsymbol{a}\right) & \boldsymbol{P}_{\mathrm{nc}}\left(\boldsymbol{a}\right) & -\left(\boldsymbol{KD}\right)^{\mathrm{T}} & \cdot & \cdot \\ \cdot & \boldsymbol{T}_{\mathrm{cc}} & \cdot & \cdot & \cdot \\ l\boldsymbol{KD} & \cdot & L_{\mathrm{ew}}\boldsymbol{KK}^{\mathrm{T}} & \cdot & \cdot \\ \cdot & \cdot & \cdot & \boldsymbol{I} & \cdot \\ \cdot & \cdot & \cdot & \cdot & -L_{\mathrm{sc}}\boldsymbol{I}\end{bmatrix}. \quad (34)$$

The resulting system (29) for the time derivative of the FE solution is independent of the chosen time-integration method, as long as the method provides continuity of the first derivative of the solution in the collocation points. In case of a rotating machine, also the time derivative of the stiffness matrix $\boldsymbol{S}$ needs to be calculated.

IV. Results

The proposed method was first tested in case of the TR rule. The simulation parameters were equal to those in Section II C. The instantaneous powers and power balance are shown in Fig. 3. The input power and stator resistive losses do not depend on the derivative of the solution and are thus equal to those in Fig. 2 b). However, more accurate calculation of the cage losses and the rate-of-change of the field energy now allows satisfying the power balance.

Fig. 4 shows the effect of the time-step length on the absolute value of the power balance, eddy-current losses and rate-of-change of the field energy averaged over the first tenth of a period by summing up the powers in the collocation points. The proposed method and the BWD method for the calculation of the derivative are compared. The proposed method satisfies the power balance in the collocation points very well with different time-step lengths. In addition, when the time step is shortened, the average powers obtained with the proposed method converge faster than those obtained with the BWD approximation.

The continuous solution (21) obtained with the collocation method allows studying the power balance also during the time steps. Fig. 5 shows the continuous powers and power balances obtained both with the TR rule and the IM rules. It is clearly seen that the TR rule provides continuity of the derivative of the solution from one time step to another thus also making the cage losses, the rate-of-change of the field energy and the power balance continuous. On the other hand, the IM method provides only a linear approximation for the solution and thus the two powers and the power balance are not continuous at the end points. However, also in this case, the power balance is satisfied in the collocation points.

V. Discussion

A method for accurate calculation of the time derivative of an FE solution based on the collocation method and differentiation of the constraint equations was described. Unlike the commonly-used backward-difference approximation, the proposed method allows calculating the instantaneous powers related to the variation of the magnetic field and conductor currents accurately in the collocation points.

Derivation of the time-integration methods using the collocation approach also helps to understand how the solution actually behaves during the time step and at which instants the system equation and the power balance are satisfied. This knowledge can later be used to study how the instantaneous powers should be integrated in order to obtain the energy balance of the machine accurately.

One application for the proposed method is power balanced torque computation of a rotating machine. However, in this case, differentiation of the constraint equations requires differentiation of the system matrix, which strongly depends on the method chosen for modeling the motion of the rotor.

Acknowledgment

The Academy of Finland is acknowledged for financial support.

References

[1] A. Arkkio, A. Hannukainen, "Proper finite-element discretization for torque computation of cage induction motors," in *Proc. SPEEDAM*, 2012, pp. 1456-1461.

[2] J. L. Coulomb, "A Methodology for the Determination of Global Electromechanical Quantities from a Finite Element Analysis and Its Application to the Evaluation of Magnetic Forces, Torques and Stiffness," *IEEE Trans. Magn.*, Vol. 19, No. 6, pp. 2514-2519, November 1983.

[3] M. Marinescu, N. Marinescu, "Numerical Computation of Torques in Permanent Magnet Motors by Maxwell Stresses and Energy Method," *IEEE Trans. Magn.*, Vol. 24, No. 1, pp. 463-466, January 1988.

[4] A. Brambilla, D. D'Amore, "Energy-Based Control of Numerical Errors Time-Domain Simulation of Dynamic Systems," *IEEE Trans. Circuits Syst. I, Fundam. Theory Appl.*, Vol. 48, No. 5, pp. 543-551, May 2001.

[5] D. Eberard, B. M. Maschke, A. J. van der Schaft, "Energy-conserving formulation of RLC-circuits with linear resistors," in *Proc. International Symposium on Mathematical Theory of Networks and Systems*, Kyoto, Japan, 2006.

[6] R. Rieben, D. White, G. Rodrigue, "High-Order Symplectic Integration Methods for Finite Element Solutions to Time Dependent Maxwell Equations," *IEEE Trans. Antennas Propag.*, Vol. 52, No. 8, pp. 2190-2195, August 2004.

[7] E. Dlala, A. Belahcen, A. Arkkio, "On the Importance of Incorporating Iron Losses in the Magnetic Field Solution of Electrical Machines," *IEEE Trans. Magn.*, Vol. 46, No. 8, pp. 3101-3104, August 2010.

[8] D. Lin, P. Zhou, Q. M. Chen, N. Lambert, Z. J. Cendes, "The Effects of Steel Lamination Core Losses on 3D Transient Magnetic Fields," *IEEE Trans. Magn.*, Vol. 46, No. 8, pp. 3539-3542, August 2010.

[9] J. Pippuri, "Finite Element Analysis of Eddy Current Losses in Steel Laminations of Inverter-Fed Electrical Machines," Ph.D. thesis,

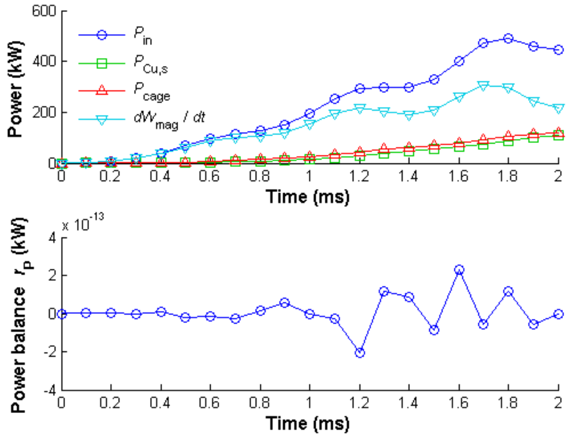

Integration with TR, derivative with proposed method

Fig. 3 End-point powers and power balances for the induction machine calculated with the proposed method while using the TR rule for the time integration.

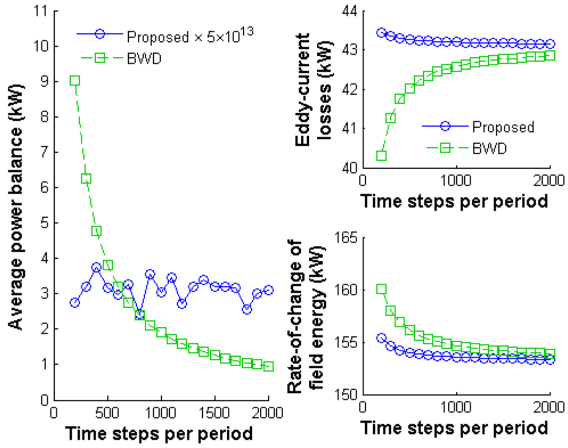

Fig. 4 Effect of time-step length on the absolute value of the end-point power balances and powers averaged over 1/10 period with both the proposed and BWD methods while using the TR rule for the time integration.

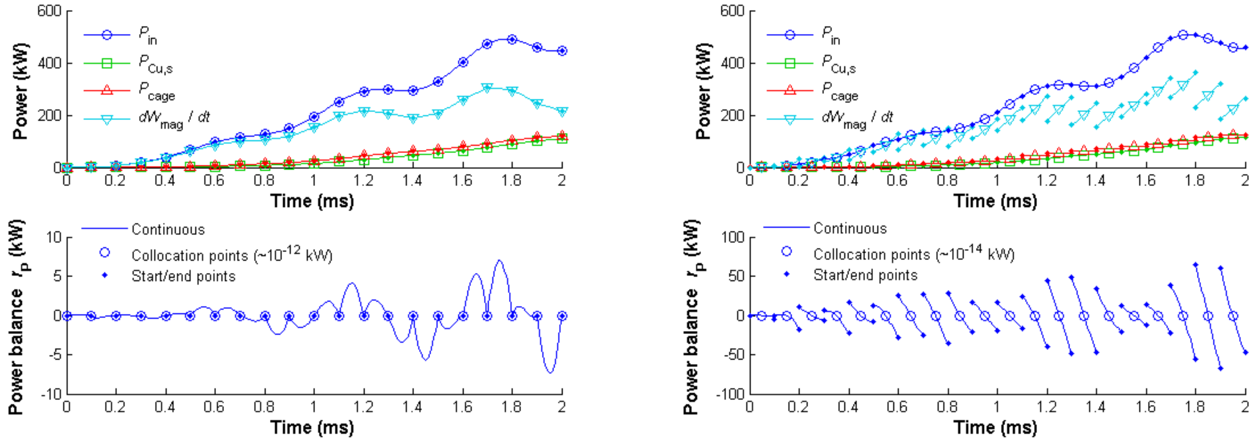

a) TR rule

b) IM rule

Fig. 5 Continuous powers and power balances in case of a) the TR rule and b) the IM rule. The markers denote the values at the collocation points and the dots at the start and end points of the time steps.

Helsinki University of Technology, 2010. Available at http://lib.tkk.fi/Diss/2010/isbn9789526034263/isbn9789526034263.pdf.

[10] P. Rasilo, A. Belahcen, A. Arkkio, "Importance of Iron-Loss Modeling in Simulation of Wound-Field Synchronous Machines," *IEEE Trans. Magn.*, Vol. 48, No. 9, pp. 2495-2504, September 2012.

[11] S. L. Ho, S. Niu, W. N. Fu, J. Zhu, "A Power-Balanced Time-Stepping Finite Element Method for Transient Magnetic Field Computation," *IEEE Trans. Magn.*, Vol. 28, No. 2, pp. 291-294, February, 2012.

[12] E. Hairer, C. Lubich, G. Wanner, "Geometric Numerical Integration – Structure-Preserving Algorithms for Ordinary Differential Equations," Springer, Berlin, 2002.

[13] W. N. Fu, S. L. Ho, "Instantaneous Power Balance Analysis in Finite-Element Method of Transient Magnetic Field and Circuit Coupled Computation," *IEEE Trans. Magn.*, Vol. 49, No. 5, pp. 1561-1564, May 2013.

[14] D. G. Dorrell, M. Popescu, M. I. McGilp, "Torque Calculation in Finite Element Solutions of Electrical Machines by Consideration of Stored Energy," *IEEE Trans. Magn.*, Vol. 42, No. 10, pp. 3431-3433, October 2006.

[15] S. Niu, S. L. Ho, W. N. Fu, "Power Balanced Electromagnetic Torque Computation in Electric Machines Based on Energy Conservation in Finite-Element Method," *IEEE Trans. Magn.*, Vol. 49, No. 5, pp. 1561-1564, May 2013.

[16] P. Kunkel, V. Mehrmann, "Differential-algebraic equations: analysis and numerical solution," European Mathematical Society, Berlin 2006.

[17] R. de P. Soares A. R. Secchi, "Direct Initialisation and solution of High-Index DAE Systems," Computer Aided Chemical Engineering, Vol. 20, Part A, pp. 157-162, 2005.

[18] A. Arkkio, "Analysis of Induction Motors Based on the Numerical Solution of the Magnetic Field and Circuit Equations," Ph.D. thesis, Helsinki University of Technology, 1987. Available at http://lib.tkk.fi/Diss/198X/isbn951226076X/.

[19] U. M. Asher, L. R. Petzold, "Computer Methods for Ordinary Differential Equations and Differential-Algebraic Equations," SIAM, 1998.